

Investigation on Mechanism of Steel Bar Corrosion of Reinforced Concrete Structures in Aqueous Solution Using Wenner Technique

Charles Kennedy¹, Bright Akoba², Irimiagha Paul Gibson³

¹Faculty of Engineering, Department of Civil Engineering, Rivers State University, Nkpolu, Port Harcourt, Nigeria.

^{2,3}School of Engineering, Department of Electrical / Electronics Engineering, Kenule Beeson Saro-Wiwa Polytechnic, Bori, Rivers State, Nigeria.

Authors E-mail: ¹ken_charl@yahoo.co.uk, ²brightakoba813@gmail.com, ³mie4tammy@gmail.com

Abstract

This experimented work investigated the electrochemical processed that led to the electron transfer in corrosion process of steel reinforcement in the harsh marine environment with high level of chloride. Corrosion test was conducted on high tensile reinforcing steel bar of 12mm, specimens rough surface were treated with Symphonia globulifera linn resin extracts with layered thickness of 150 μ m, 250 μ m and 350 μ m polished and embedded into concrete slab. Specimens of control, non-inhibited and resin inhibited specimens were cured for initial 28 days and corrosion acceleration process with Sodium Chloride lasted for 119days with 14 days checked intervals for readings. Results recorded of half cell potential, concrete resistivity and tensile strength properties for non- inhibited concrete specimens on the mapping areas for the expedited periods designated 95% probability of corrosion and betokening a high or moderate probability of corrosion. Average results on comparison showed incremental values of 70.1% against 27.2% non-corroded of potential and 87.8% to 38.8% decremented values in concrete resistivity, yield stress against ultimate strength at summary and average state of corroded slab with nominal values of 100% and decremented in ultimate strength from 100.68% to 96.12%, weight loss versus cross-section diameter reduction decremented due to assail from sodium chloride from 67.1% to 48.5% and 98.2% to 94.82% respectively. Average percentile results of potential and concrete resistivity are 29.9% and 63.6% respectively. When compared to corroded samples, corroded has 70.1% incremented values potential E_{corr},mV and 38.8% decremented values of concrete resistivity, yield stress against ultimate vigor at in comparison to corrode as 100% nominal yield stress decremented from 103.06% to 96.12% and weight loss at 67.5% against 48.5% and 47.80% to 94.82% cross-sectional diameter reduction, both showed decremented values of corroded compared to coated specimens.

Key Words: Corrosion, Corrosion inhibitors, corrosion potential, concrete resistivity and Steel

Reinforcement

1.0 Introduction

The process of corrosion is electrochemical, it is a chemical reaction involving the transfer of electrons from one specimen to another. An electrochemical cell consists of two electrodes known as cathode and anode that involved in a corrosion reaction. These electrodes are placed in an aqueous solution, by joining both electrodes electrically. Fontana [1]. Steel reinforcement in concrete is normally immune from corrosion due to high alkalinity of concrete, however, steel corrodes when attacked by aggressive agents. These two mechanisms usually do not attack the integrity of concrete but they attack steel bars. However, other ions such as sulfates attack the integrity of concrete before attacking the steel, Broomfield 1997 [2]. The presence of chloride in sufficient concentration at steel concrete interface causes damage to reinforcement by attacking the passive layer. In electrochemical cells an external source of power is used to drive current through the system and hence there is a shift of electrode potential from its equilibrium value which is called polarization (Uhlig and Revie [3], Rosenberg *et al.* [4]).

Chemical reactions occur between the different phases at the inter-phase surface while the transport processes transmit the reactions to the surface and withdraw the reaction products. The transport process and ingress of moisture or aggressive agents and air which result in the chemical reactions and consequent concrete deterioration are controlled the permeability of concrete. Neville [5] defined the permeability of a medium which characterizes the ease with which a fluid will pass through the medium under the action of a pressure differential and therefore, it represents the relative ease with which concrete can become saturated with water. It is generally believed that some chloride ions can react chemically with a calcium aluminate mineral in the cement gel and therefore, tricalcium aluminates (C_3A) amount of the cement

has a strong influence on the amount of chlorides remaining in the hydrated cement paste pore solution (Suryavanshi *et al.* [6],

Blend agents (slag, pozzolans and fillers) can influence the permeability and therefore the rate of penetration of chloride ions (Thomass [7], Vedalakshmi *et al.* [8]). Blending cement with blast furnace slag has been found to reduce the diffusion rate of chloride ions (Dehghanian and Arjemandi [9], Song [10]). Also it was reported by Cabrera [11]; Alexander and Magee [12] that the uses of silica fume in concrete reduce concrete permeability, improve durability and lower the penetration rate of chloride. The effect of fly ash (Up to 50%) on concrete samples under immersion in chloride has been studied by Montemor, *et al.* [13], Saraswathy and Song [14]. It was found that fly ash reduces chloride diffusion and decreases the corrosion rate.

2.0 MATERIALS AND METHODS FOR EXPERIMENT

2.1 Aggregates

The fine aggregate and coarse aggregate were purchased. Both met the requirements of [15]

2.1.2 Cement

The cement used was Ordinary Portland Cement, it met the requirements of [16]

2.1.3 Water

The water samples were clean and free from impurities. The fresh water used was gotten from the tap at the Civil Engineering Department Laboratory, Kenule Beeson Polytechnic, Bori, Rivers State. The water met the requirements of [17]

2.1.4 Structural Steel Reinforcement

The reinforcements are gotten directly from the market in Port Harcourt. [18]

2.1.5 Corrosion Inhibitors (Resins / Exudates) *Symphonia globulifera linn*

The study inhibitor *Symphonia globulifera* linn is of natural tree resins /exudates substance extracts.

2.2 EXPERIMENTAL PROCEDURES

2.2.1 Experimental method

2.2.2 Sample preparation for reinforcement with coated resin/exudates

Corrosion test was conducted on high tensile reinforcing steel bar of 12mm, specimens rough surface were treated with sandpaper and wire brush, washed with acetone to remove rust and dried to enable proper adhesion of coated / inhibitive materials. Coating was done by direct application on the ribbed reinforcement rough surface with 150 μ m, 250 μ m and 350 μ m coated thicknesses of *Symphonia globulifera* linn paste were polished and allowed to dry for 72 hours before embedded into concrete slab.

Mix ratio of 1:2:3 by weight of concrete, water cement ratio of 0.65, and manual mixing was adopted. The samples were designed with sets of reinforced concrete slab of 150mm thick x 350mm width x 900mm long, uncoated and coated specimens of above thicknesses were embedded into the concrete, spaced at 150mm apart. Fresh concrete mix batch were fully compacted to remove trapped air, with concrete cover of 15mm and projection of 150mm for half cell potential measurement and concrete resistivity tests. Slabs were demoulded after 72 hours and cured for 28 days with room temperature and corrosion acceleration ponding process with Sodium Chloride lasted for 119days with 14 days checked intervals for readings. The corrosion rates were quantified predicated on current density obtained from the polarization curve and the corrosion rate quantification set-up. The corrosion cell consisted of a saturated calomel reference electrode (SCE), counter electrode (graphite rod) and the reinforcing steel embedded in concrete specimen acted as the working electrode. The polarization test was performed utilizing scanning potential of -200 mV through 1200mV, with a scan rate of 1mV/s. The data were recorded for a fine-tuned duration of 1hr at ambient temperature. The polarization curve was obtained as the relationship between corrosion potential and current density.

2.3 Accelerated Corrosion Test

In order to test concrete resistivity and durability against corrosion, it was necessary to design an experiment that would accelerate the corrosion process and maximize the concrete's resistance against corrosion until failure. The accelerated corrosion test allows the acceleration of corrosion to reinforcing steel embedded in concrete and can simulate corrosion growth that would occur over decades. A laboratory acceleration process helps to distinguish the roles of individual factors that could affect chloride induced corrosion. An accelerated corrosion test is the impressed current technique which is an effective technique to investigate the corrosion process of steel in concrete and to assess the damage on the concrete cover. (Care and Raharinaivo [19]) Reinforcement corrosion normally requires long exposure period of time, and usually by the first crack observed on the concrete surface. Therefore, for design of structural members and durability against corrosion as well as selection of suitable material and appropriate protective systems, it is useful to perform accelerated corrosion tests for obtaining quantitative and qualitative information on corrosion resistance in a relatively shorter period of time.

2.4 Corrosion Current Measurements (Half-cell potential measurements)

Half-cell potential measurements are indirect method of assessing potential bar corrosion, but there has been much recent interest in developing a means of performing perturbative electrochemical measurements on the steel itself to obtain a direct evaluation of the corrosion rate (Gowers and Millard [20]). Corrosion rates have been related to electrochemical measurements based on data first reported by Stern and Geary [21]. If the potential measurements indicate that there is a high probability of active corrosion, concrete resistivity measurement can be subsequently used to estimate the rate of corrosion. This was also stated from practical experience (Figg and Marsden [22] and Langford and Broomfield [23]). Classifications of the severity of rebar corrosion rates are presented in Table 2.1. However, caution needs to be exercised in using data of this nature, since constant corrosion rates with time are assumed.

Table 2.1: Dependence between potential and corrosion probability

Potential E_{corr}	Probability of corrosion
$E_{\text{corr}} < -350\text{mV}$	Greater than 90% probability that reinforcing steel corrosion is occurring in that area at the time of measurement
$-350\text{mV} \leq E_{\text{corr}} \leq -200\text{mV}$	Corrosion activity of the reinforcing steel in that area is uncertain
$E_{\text{corr}} > -200\text{mV}$	90% probability that no reinforcing steel corrosion is occurring in that area at the time of measurement (10% risk of corrosion)

2.5 Concrete Resistivity Measurement Test

In the study, the Wenner four probes method was used, it was done by placing the four probes in contact with the concrete directly above the reinforcing steel bar. Different readings were taken at different locations at the surface of the concrete. The mean values of the readings were recorded as the final readings of the resistivity in the study. The saturation level of the slabs was monitored through concrete electrical resistivity measurements, which are directly related to the moisture content of concrete. The electrical resistivity becomes constant once the concrete has reached saturation. Before applying water on the slabs, the concrete electrical resistivity was measured in the dry condition at the specified locations. Henceforth, these measurements will be referred to as the measurements in «dry» conditions. These locations were chosen at the side of the slabs, since concrete electrical resistivity measurements could be taken when water was on the top surface of the slab. Time limitation was the main challenge to perform all the experimental measurements, as the concrete saturation condition changes with time. After applying water on the surface of the slabs, the concrete resistivity was measured daily at the reference locations, looking for the saturation condition. Since each of the slabs had a different w/c, the time needed to saturate each of the slabs was not the same. Once one slab would reach the saturated condition, the water could be drained from that slab, while the other slabs remained ponded.

Table 2.2: Dependence between concrete resistivity and corrosion probability

Concrete resistivity ρ , k Ω cm	Probability of corrosion
$\rho < 5$	Very high
$5 < \rho < 10$	High
$10 < \rho < 20$	Low to moderate
$\rho > 20$	Low

2.6 Tensile Strength of Reinforcing Bars

To ascertain the yield and tensile strength of tension bars, bar specimens of 12 mm diameter of non-corroded, corroded and coated were tested in tension in a Universal Testing Machine and were subjected to direct tension until failure; the yield, maximum and failure loads being recorded. To ensure consistency, the remaining cut pieces from the standard length of corroded and non-corroded steel bars were subsequently used for mechanical properties of steel.

3.0 Experimental results and discussion

The results of the half-cell potential measurements in table 3.1 were plotted against concrete resistivity of table 3.2 for easy interpretation. It is evident that potential E_{corr} if low (< -350 mV) in an area measuring indicates a 95% probability of corrosion. In the other measuring points,

potential E_{corr} is high ($-350\text{mV} \leq E_{\text{corr}} \leq -200\text{mV}$), which indicates a 10% or uncertain probability of corrosion

Results of the concrete resistivity measurements are shown in Table 3.2. It used as indication of likelihood of significant corrosion ($\rho < 5$, $5 < \rho < 10$, $10 < \rho < 20$, $\rho > 20$) for Very high, High, Low to moderate and Low, for Probability of corrosion. Resistivity survey data gives an indication of whether the concrete condition is favorable for the easy movements of ions leading to more corrosion. Concrete resistivity is commonly measured by four-electrode method.

3.1 Non-corroded Concrete Slab Members

Results obtained from table 3.1 of half-cell potential quantifications for and concrete resistivity for 7 days to 119 days respectively designated a 10% or skeptical probability of corrosion which denotes no corrosion presence or likelihood and concrete resistivity which denoted a low probability of corrosion or no corrosion clue.

Tables 3.1, 3.2 and tables 3.3 are the results of average values derived from desultorily slab samples from A-I of control, corroded and coated specimens of $150\mu\text{m}$, $250\mu\text{m}$, $350\mu\text{m}$ summarized to A, B and C from ABC, DEF and GHI. Figures 3.1 and 3.2 are the plots representations of Concrete Resistivity ρ , $\text{k}\Omega\text{cm}$ versus Potential E_{corr} , mV Relationship which showed average of 27.2% Potential E_{corr} , mV and 87.8% Concrete Resistivity. Figure 3.3 and 3.4 are the plots of yield stress and ultimate strength of mechanical properties of non-corroded specimens at 100.3% and 100.68%, while figures 3.5 and 3.6 are the plots of weight loss versus cross-section diameter reduction at 67.1% and 98.2% respectively.

3.2 Corroded Concrete Slab Members

Tables 3.1, 3.2 and 3.3 are the results recorded of potential E_{corr} , mV , and concrete resistivity and tensile strength properties for non-inhibited concrete specimens on the mapping areas for the expedited periods of 7 days to 119 days which designated 95% probability of corrosion and betokening a high or moderate probability of corrosion. Average results on comparison showed incremental values of 70.1% against 27.2% non-corroded of Potential E_{corr} , mV and 87.8% to 38.8%, decreased values in concrete resistivity. Figures 3.1 and 3.2 are the plots representations of concrete resistivity ρ , $\text{k}\Omega\text{cm}$ versus Potential E_{corr} , mV Relationship. Figures 3.3 and 3.4 are the plots of yield stress against ultimate vigor at summary and average state of corroded slab with nominal values of 100% and decremented in ultimate vigor from 100.68% to 96.12%, while

figures 3.5 and 3.6 presented the weight loss versus cross-section diameter reduction decremented due to assail from sodium chloride from 67.1% to 48.5% and 98.2% to 94.82% respectively.

3.3 Symphonia globulifera linn Steel Bar Coated Concrete Cube Members

Tables 3.1, 3.2 and 3.3 are the results recorded of potential $E_{corr, mV}$, and concrete resistivity and tensile strength of Symphonia globulifera linn inhibited specimen, the results betokened a 10% or dubious probability of corrosion which denotes no corrosion presence or likelihood and concrete resistivity designated a low probability of corrosion or no corrosion denotement. Average percentile results of potential $E_{corr, mV}$, and concrete resistivity are 29.9% and 63.6% respectively. When compared to corroded samples, corroded has 70.1% incremented values potential $E_{corr, mV}$ and 38.8% decremented values of concrete resistivity. Figures 3.1 and 3.2 are the plots representations of Concrete Resistivity $\rho, k\Omega cm$ versus Potential $E_{corr, mV}$ Relationship. Figures 3.3 and 3.5 represented the plots for arbitrarily and computed percentile average values of yield stress against ultimate strength at in comparison to corrode as 100% nominal yield stress decremented from 103.06% to 96.12% and figures 3.5 and 3.6 respectively presented weight loss at 67.5% against 48.5% and 47.80% to 94.82%, cross-sectional diameter reduction, both showed decremented values of corroded compared to coated specimens.

Table 3.1 : Potential E_{corr} , after 28b days curing and 119 days acceleration Ponding

s/no	Inhibitor (resin/exudates) and controlled sample	Potential $E_{corr, mV}$								
		Time Intervals after 28 days curing								
		A (7days)	B (21days)	C (35days)	D (49days)	E (63days)	F (77days)	G (91days)	H (105 days)	I (119 days)
1	Control Concrete slab	-102	-102.2	-100.3	-101.2	-101.7	-100.8	-100.3	-101.4	-100.4
2	Non-inhibitor	-268.5	-294.7	-328.6	-367.7	-377.5	-384.5	-418.4	-425.6	-429.7
		150 μm ,			250 μm ,			350 μm ,		
3	Symphonia	-113.5	-117.4	-111.9	-115.5	-111.6	-118.6	-111.7	-118.2	-109.7

	globulifera linn								
Average values Potential $E_{corr,mV}$									
		ABC = A	DEF = B			GH1 = C			
1A	Control Concrete slab	-101.5	-102.2			-100.7			
2A	Non-inhibitor	-297.3	-393.5			-424.6			
		150 μ m,	250 μ m,			350 μ m,			
3A	Symphonia globulifera linn	-114.3	-115.2			-113.2			

Table 3.2 : Results of Concrete Resistivity ρ , $k\Omega$ cm Time Intervals after 28 days curing curing and 119 days acceleration ponding

s/no	Inhibitor (resin/exudates) and controlled sample	Concrete Resistivity ρ, $k\Omega$cm								
		Time Intervals after 28 days curing								
		A (7days)	B (21days)	C (35days)	D (49days)	E (63days)	F (77days)	G (91days)	H (105 days)	I (119 days)
1	Control Concrete slab	15.35	15.52	15.42	15.65	15.48	14.43	15.45	15.45	15.48
2	Non-inhibitor	6.77	6.91	7.74	8.05	8.22	8.38	9.12	9.55	9.59
		150 μ m,			250 μ m,			350 μ m,		
3	Symphonia globulifera linn	13.26	13.29	13.46	14.24	14.18	14.23	14.39	14.45	14.78
Average values Concrete Resistivity ρ, $k\Omega$cm										

		ABC = A	DEF = B	GH1 = C
1B	Control Concrete slab	15.43	15.19	15.46
2B	Non-inhibitor	7.14	8.21	9.42
3B		150µm,	250µm,	350µm,
	Symphonia globulifera linn	13.34	14.22	14.54

Table 3.3 : Mechanical properties of Non-Corroded, Corroded and Coated Beam

s/no	Inhibitor (resin/exudates) and controlled sample	Yield Stress (N/mm ²)								
		Time Intervals after 28 days curing								
		A (7days)	B (21days)	C (35days)	D (49days)	E (63days)	F (77days)	G (91days)	H (105 days)	I (119 days)
1	Control Concrete slab	410.4	410.1	410.3	410.0	410.3	410.7	410.0	410.5	410.4
2	Non-inhibitor	410.2	410.0	410.0	410.4	410.0	410.3	410.0	410.3	410.2
		150µm,			250µm,			350µm,		
3	Symphonia globulifera linn	410.6	410.2	410.7	410.7	410.7	410.4	410.2	410.2	410.4
		Average values Yield Stress (N/mm ²)								
		ABC = A			DEF = B			GH1 = C		
1C	Control Concrete slab	410.27			410.33			410.3		
2C	Non-inhibitor	410.01			410.23			410.17		

		150µm,			250µm,			350µm,		
3C	Symphonia globulifera linn	410.45			410.60			410.27		
Ultimate strength (N/mm²)										
1	Control Concrete slab	564.7	565.6	562.4	562.6	566.8	562.2	565.2	562.7	562.4
2	Non-inhibitor	584.7	585.8	586.8	582.8	586.8	582.8	585.4	582.6	588.4
		150µm,			250µm,			350µm,		
3	Symphonia globulifera linn	560.9	566.4	568.4	566.7	569.5	568.7	568.5	564.9	563.5
Average value of Ultimate strength (N/mm²)										
		ABC = A			DEF = B			GHI = C		
1D	Control Concrete slab	564.23			563.87			563.43		
2D	Non-inhibitor	585.77			584.13			585.47		
		150µm,			250µm,			350µm,		
3D	Symphonia globulifera linn	565.23			568.3			567.97		
Weight Loss of Steel Loss (in grams)										
1	Control Concrete slab	10.628	10.796	10.839	10.876	10.882	10.884	10.835	10.885	10.676
2	Non-inhibitor	7.25	7.37	7.33	7.25	7.26	7.45	7.28	7.18	7.35
		150µm,			250µm,			350µm,		
3	Symphonia globulifera linn	7.29	7.29	7.25	7.30	7.26	7.26	7.31	7.29	7.28

		Average values of Weight Loss of Steel Loss (in grams)								
		ABC = A			DEF = B			GH1 = C		
1E	Control Concrete slab	7.32			7.33			7.27		
2E	Non-inhibitor	10.754			10.681			10.799		
		150µm,			250µm,			350µm,		
3E	Symphonia globulifera linn	7.27			7.27			7.29		
		Cross- section Area Reduction (Diameter, mm)								
1	Control Concrete slab	12	12	12	12	12	12	12	12	12
2	Non-inhibitor	11.53	11.53	11.54	11.61	11.64	11.71	11.75	11.76	11.79
		150µm,			250µm,			350µm,		
3	Symphonia globulifera linn	12	12	12	12	12	12	12	12	12
		Average Values of Cross- section Area Reduction (Diameter, mm)								
		ABC = A			DEF = B			GH1 = C		
1F	Control Concrete slab	12			12			12		
2F	Non-inhibitor	11.587			11.563			11.662		
		150µm,			250µm,			350µm,		
3F	Symphonia globulifera linn	12			12			12		

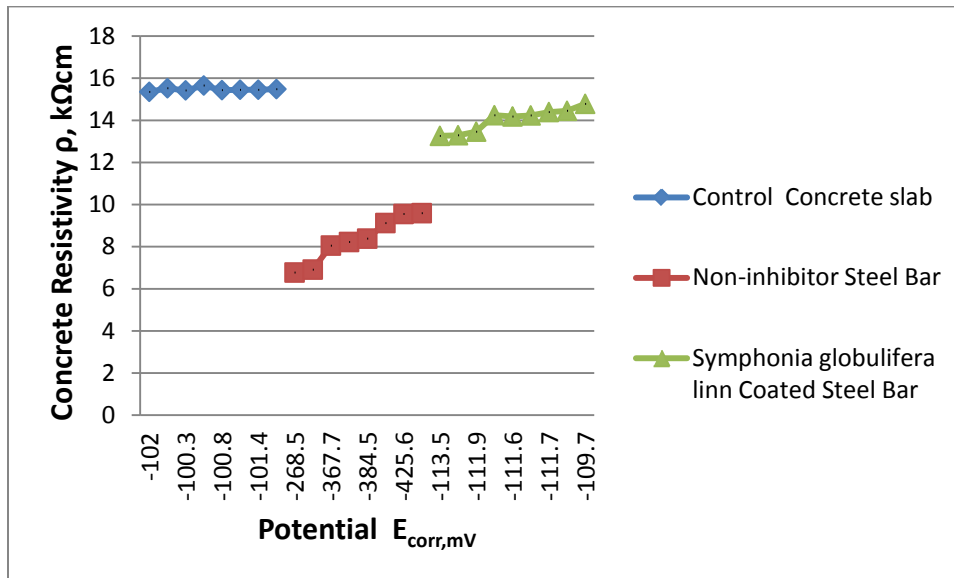


Figure 3.1: Concrete Resistivity versus Potential Relationship Concrete Resistivity ρ , kΩcm versus Potential E_{corr} , mV Relationship

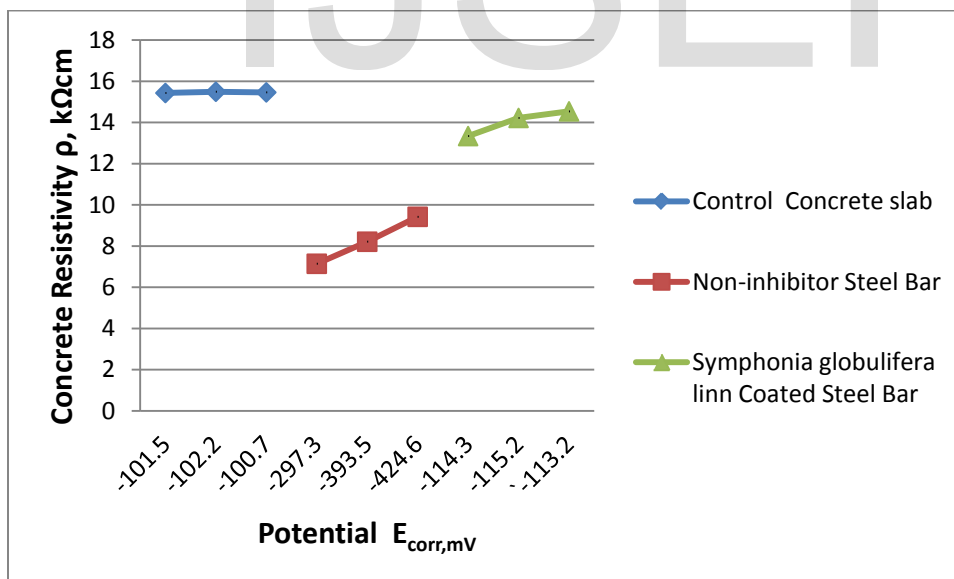


Figure 3.2: Average Concrete Resistivity versus Potential Relationship

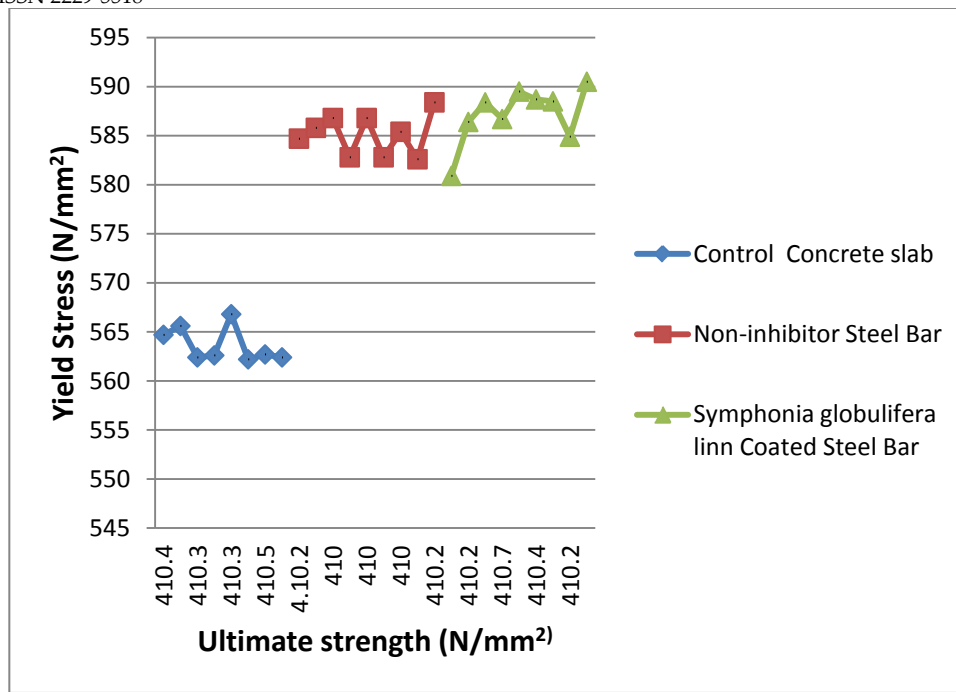


Figure 3.3: Yield Stress versus Ultimate strength.

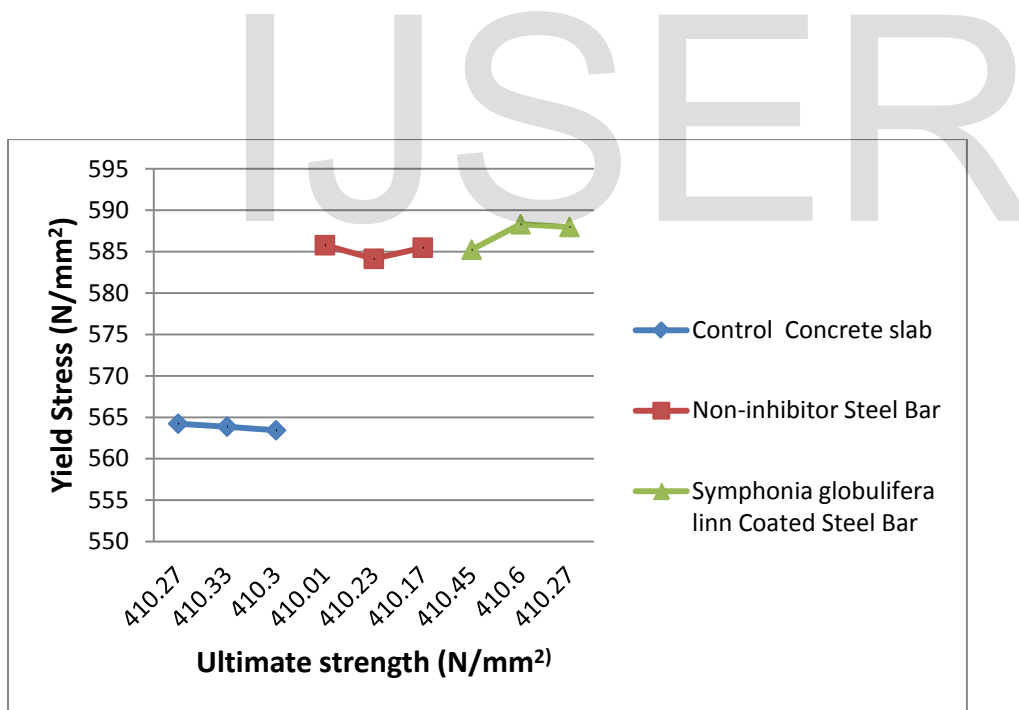


Figure 3.4: Average Yield Stress versus Ultimate strength.

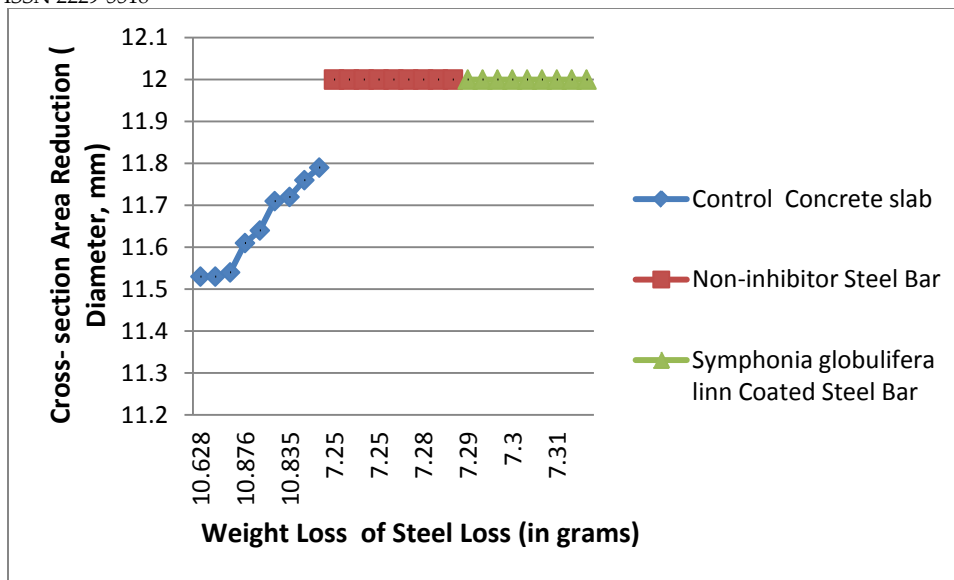


Figure 3.5: Weight Loss of Steel Loss versus Cross-section Area Reduction

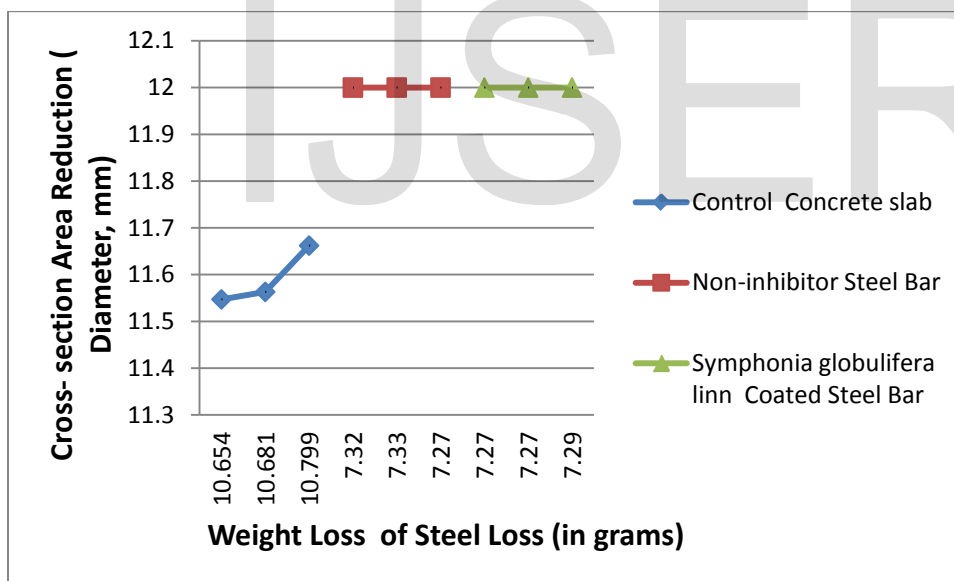


Figure 3.6: Average Weight Loss of Steel Loss versus Cross-section Area Reduction

4.0 Conclusion

Experimental results showed the following conclusions:

- i. Entire results showed lower percentages in corroded and higher in coated members.
- ii. Results justified the effect of corrosion on the strength capacity of corroded and coated members.
- iii. Results showed the effectiveness of resins extracts of tree as inhibitive materials
- iv. Resins form protective coat membrane towards corrosion effects
- v. Corroded specimens showed reduction in cross-section area of the reinforcement due to severe attacks

REFERENCES

- [1] M. G. Fontana, Corrosion Engineering. USA: McGraw-Hill Book Company, 1986.
- [2] J.G. Broomfield, "Corrosion of Steel in Concrete: Understanding, Repair and Investigation, (1st Edition), UK: E and FN Spon;" 1997.
- [3] H. Uhlig, Corrosion and Control, UK: George Harrap and Co. Ltd., 2004.
- [4] A.M. Rosenberg, and J.M. Gaidis, "Calcium Nitrite as an Inhibitor of Concrete", Material Performance, no. 18, pp. 45-51, 1979.
- [5] A.M. Neville, "Properties of Concrete, (3rd Edition), UK," Pitman, 1981.
- [6] A. K. Suryavanshi, J. D. Scantlebury, and S. B. Lyon, "Corrosion of Reinforcement Steel Embedded in High Water-Cement Ratio Concrete Contaminated With Chloride," *Cement and Concrete Composites*, no. 20, pp. 263-281, 1998.
- [7] M. Thomas, "Chloride Thresholds in Marine Concrete", *Cement and Concrete Research*, no. 26, pp. 513-519, 1996.
- [8] R.Vedalakshmi, K. Rajagopal, and N. Palaniswamy, "Long-term Corrosion Performance of Rebar Embedded in Blended Cement Concrete under Macro Cell corrosion condition", *Construction and Building Materials*, no. 22, pp. 186-199, 2008.
- [9] C. Dehghanian, and C.E. Locke, "Electrochemical Behaviour of Steel in Concrete as a result of Chloride Diffusion into Concrete: Part 2", *Corrosion*, no. 38, pp. 494-499, 1982.
- [10] H.W., Song, C. H. Lee, and K.Y. Ann, "Factors Influencing Chloride Transport in Concrete Structures Exposed to Marine Environments," *Cement and Concrete Composites*, no.30, pp. 113-121, 2008.
- [11] J.G. Cabrera, "Deterioration of Concrete due to Reinforcement Steel Corrosion", *Cement and Concrete Composites*, no. 18, pp. 47-59, 1996.
- [12] M.G. Alexander, and B. J. Magee, "Durability of Performance Concrete containing Condensed Silica Fume", *Cement and Concrete Research*, no. 29, pp. 917- 922, 1999.
- [13] M. Montemor, A. Simoes, and M. Salta, "Effect of Fly Ash on Concrete Reinforcement Corrosion Studied by Electrochemical

- Impedance Technique,” *Cement and Concrete Composites*, no. 22, pp. 175-185, 2000.
- [14] V. Saraswathy, and H. W. Song, “Studies on the Corrosion Resistance of Reinforced Steel in Concrete with Ground Granulated Blast-Furnace Slag - an overview,” *Journal of Hazardous Materials*, no. 16, pp. 226-233, 2006.
- [15] BS 882; - Specification for Aggregates from Natural Sources for Concrete, *British Standards Institute. London, United Kingdom*, 1992.
- [16] BS EN 196-6; - Methods of Testing Cement. Determination of Fineness, *British Standards Institute. London, United Kingdom*, 2010.
- [17] BS 3148 – Methods of test for water for making concrete. *British Standards Institute. London, United Kingdom*, 1980.
- [18] BS 4449:2005+A3 – Steel for Reinforcement of Concrete. *British Standards Institute. London, United Kingdom*, 2010.
- [19] S. Care, and A. Raharinaivo, “Influence of impressed current on the initiation of damage in reinforced mortar due to corrosion of embedded steel”, *Cement and Concrete Research*, no. 37, pp.1598-1612, 2007.
- [20] K. R. Gowers, and S. G., Millard, “Measurement of Concrete Resistivity for Assessment of Corrosion Severity of Steel using Wenner Technique,” *ACI Materials Journal*, vol. 96, no. 5, pp. 536-542, 1999.
- [21] M. Stern, and A. L. Geary, “Electrochemical Polarization I: Theoretical Analysis of shape of Polarization curves,” *Journal of Electrochemistry Society*, no.104, pp. 56-63, 1957. cited by Poupard *et al.*, “Characterizing Reinforced Concrete Beams Exposed During 40 years in a Natural Marine Environment - Presentation of the French Project Benchmark des Poutres de la Rance,” *proceedings of the 7th CANMET/ACI international conference on durability of concrete*, Montreal Canada, American Concrete Institute SP 134, pp. 17-30, 2006.
- [21] J. W. Figg and A.F. Marsden, “Development of Inspection Techniques for Reinforced Concrete: a State of the Art Survey of Electrical Potential and Resistivity Measurements in Concrete in the Oceans,” HMSO, London, Technical Report 10, OHT 84 205, 1985.
- [21] P. Langford and J. Broomfield, “Monitoring the Corrosion of Reinforcing Steel,” *Construction Repair*, pp. 32-36, 1987.

IJSER